THE INTERPRETATION OF LOW-ANGLE X-RAY DATA FROM PLANAR AND CONCENTRIC MULTILAYERED STRUCTURES

The Use of One-Dimensional Electron Density Strip Models

C. R. WORTHINGTON

From the Department of Physics and the Biophysics Research Division, University of Michigan, Ann Arbor, Michigan 48104

ABSTRACT The use of one-dimensional electron density strip models in interpreting low-angle X-ray data from planar and concentric multilayered structures is described. Diffraction formulas for an n-strip model are given. Fourier transforms, normalization constants, and Patterson functions are derived for certain strip models.

INTRODUCTION

Planar and concentric multilayered structures have a wide spread occurrence in biology. Retinal rods, mitochondria, and collagen are examples of planar multilayered structures whereas nerve myelin is an example of a concentric multilayered structure. Discrete low-angle X-ray diffraction is observed because these structures have large unit cells and also have well-defined repeating units; linear repeats for the planar structures and a radial repeat for nerve myelin.

In a previous paper (Blaurock and Worthington, 1966) the treatment of low-angle X-ray data from these structures was considered. The relation between the integrated intensity $I(h)$ and the Fourier transform of the unit cell $T(h)$ was given:

$$I(h) \alpha \Delta(h) | T(h)|^2 \quad (1)$$

where the function $\Delta(h)$ is different for planar and radial repeats and makes allowance for the transverse size of the structures and also for the divergence of the X-ray beam. In this paper, it is assumed that $\Delta(h)$ is known and hence, if the proportionality constant α is also known, a set of $J(h) = | T(h)|^2$ is obtained.

Experimentally we can only record a set of observed intensities $J_{obs}(h)$ on a relative scale compared to $J(h)$ which is said to be on an absolute scale. Our set of

$J_{obs}(h)$ does not include the zero order $h = 0$. Furthermore, in low-angle X-ray studies the experimental problem of recording a large number of diffraction orders is a formidable one and in practice only a limited set of $J_{obs}(h)$ is obtained. We require a structural interpretation of our observed intensities $J_{obs}(h)$.

A problem of current interest is to describe membrane structure in terms of component electron densities, that is, in terms of uniform electron density layers parallel to the membrane surface. This description of the membrane structure in terms of uniform electron densities within layers or strips describes an electron density strip model. Low-angle X-ray data is available from either intact biological membranes or an orderly arrangement of biological membranes prepared by sedimenting in the ultracentrifuge (for example, Blasie et al., 1965). In some instances, structural interpretations have been attempted on the basis of an electron density strip model. For example, an electron density model of nerve myelin which, to some extent, rests on the knowledge of the electron density of the medium between the membrane pair has been proposed by Worthington and Blaurock (1968). Another way to propose a model is on the basis of the electron densities of the components thought to comprise the membrane. This approach has been followed by Rand and Luzzati (1968) for the lipids extracted from human erythrocytes. In any case, no matter how the model is derived, the use of electron density strip models is one way to account for the observed low-angle X-ray data.

The purpose of this study is to point out the usefulness of electron density strip models in interpreting the low-angle X-ray data from planar and concentric multilayered structures. Diffraction formulas for the one-dimensional strip models are derived. Some simplified membrane-type models are examined in more detail and criteria are given which could lead to the choice of such a model for interpreting the low-angle X-ray data from biological membranes.

REVIEW OF DIFFRACTION FORMULAS

Let $t(x)$ represent the electron density variation of a single unit cell of length d along the fiber axis (axis at right angles to the planar surface) for planar structures or along the radial axis for concentric structures. In this paper only the centrosymmetric case will be treated; we assume $t(x)$ to be centrosymmetric, that is, $t(x) = t(-x)$. $t(x)$ and $T(X)$ are a pair of Fourier transforms, denote $t(x) \rightleftharpoons T(X)$ where

$$T(X) = \int_0^d t(x) \cos 2\pi Xx \, dx, \tag{2}$$

$$t(x) = \int_{-\infty}^{\infty} T(X) \cos 2\pi Xx \, dx, \tag{3}$$

and where x, X are direct and reciprocal space coordinates. The low-angle X-ray diffraction maxima occur at $X = h/d$, that is, $T(X)$ is sampled at intervals of $1/d$

by the interference function of a linear array of unit cells so that $t(x)$ has a Fourier series representation.

There are three Fourier series representations for the electron density variation, these are $t(x)$, $t'(x)$ and $t''(x)$:

$$t(x) = 1/d\sum_{-\infty}^{\infty} T(h) \cos 2\pi hx/d, \tag{4}$$

$$t'(x) = 1/d\sum_{-h}^{h} T(h) \cos 2\pi hx/d, \tag{5}$$

$$t''(x) = 2/d\sum_{1}^{h} \{\pm\}[J_{obs}(h)]^{1/2} \cos 2\pi hx/d, \tag{6}$$

where $\{\pm\}$ is the phase information. The first representation equation (4) is the original $t(x)$, the second equation (5) differs from the original because of series termination, whereas the third representation equation (6) is on a relative scale, the zero order term is missing, and it also suffers from series termination.

The series termination effect arises from only recording finite h (James, 1948). This is equivalent to a reciprocal space cut off X_o where X_o = (maximum value of h)/d. The integral in equation 3, therefore, has limits $\pm X_o$. Define a window function $W(X)$ which has value unity within the range $-X_o \leq X \leq X_o$ and zero outside this range. Denote $w(x) \rightleftharpoons W(X)$ where $w(x) = 2X_o$ sinc $2\pi X_o x$ and where sinc θ = sin θ/θ. Then, it follows that $t'(x)$ is given by

$$t'(x) = t(x) * w(x) \tag{7}$$

where $*$ is the convolution symbol.

The observed intensities $J_{obs}(h)$ can be converted to an absolute scale by use of the normalization constant K. Because $J_{obs}(h)$ does not include the zero-order term the following notation is used: $J(h) = J(0) + J'(h)$ and similarly $T(h) = T(0) + T'(h)$ where $J'(h)$ and $T'(h)$ contain non-zero integral values of h. We define $KJ_{obs}(h) = J'(h)$. In order to work on an absolute scale, the knowledge of the normalization constant K and also the value of $J(0)$ is required.

The three Fourier series are related as follows:

$$t'(x) = t(x) * w(x) = 1/d[J(0)^{1/2} + [K]^{1/2}t''(x). \tag{8}$$

The Patterson function (James, 1948) can be directly evaluated without any phase information and a study of this function can sometimes lead to the choice of model parameters. The Patterson function $P(x)$ is defined as follows:

$$P(x) = t(x) * t(-x), \tag{9}$$

and in our notation $P(x) \rightleftharpoons J(X)$. There are three Patterson series $P(x)$, $P'(x)$,

and $P''(x)$:

$$P(x) = 1/d\sum_{-\infty}^{\infty} J(h) \cos 2\pi hx/d, \tag{10}$$

$$P'(x) = 1/d\sum_{-h}^{h} J(h) \cos 2\pi hx/d, \tag{11}$$

$$P''(x) = 2/d\sum_{1}^{h} J_{obs}(h) \cos 2\pi hx/d. \tag{12}$$

The three Patterson series are related as follows:

$$P'(x) = P(x) * w(x) = 1/dJ(0) + KP''(x). \tag{13}$$

ELECTRON DENSITY STRIP MODELS IN STRUCTURE ANALYSIS

In order to give some structural interpretation to $J_{obs}(h)$ there are two well-known approaches which can be adopted. These are the Fourier synthesis and the model approach. In the Fourier synthesis approach: determine the phase and compute a Fourier series representation, either $t'(x)$ or $t''(x)$. In the model approach: propose a model and test its correctness by comparing the $J_{obs}(h)$ values with the calculated values.

The Fourier synthesis approach requires a knowledge of the phases. Phases may be determined by use of heavy atoms or from either swelling or shrinkage phenomena (Lipson and Cochran, 1953). In low-angle X-ray studies, phases are not easily obtained. Therefore the phase problem constitutes a definite limitation to the Fourier synthesis approach, but even if the phase-problem could be solved, there is still the problem of interpreting the Fourier synthesis in terms of electron densities on an absolute scale. In previous work, when the Fourier synthesis approach was used, phases were deduced on the basis of a model (Tomlin and Worthington, 1956) or from measurements of optical density in electron micrographs (Burge and Draper, 1965, 1967). The resulting Fourier syntheses have limited resolution due to finite h. Two examples are noted: the Fourier series for collagen (Tomlin and Worthington, 1956) and the Fourier series for the cell wall of *Proteus vulgaris* (Burge and Draper, 1967); both Fouriers refer to $t''(x)$ given by equation 6. From equation 8 we see that there is still the problem of interpreting the Fourier synthesis in terms of electron densities on an absolute scale. In view of the limited resolution in the Fourier series representation for $t''(x)$ and in the absence of absolute electron density information, one usually attempts to deduce some electron density strip model from $t''(x)$ which can then be tested with the $J_{obs}(h)$ data. Hence the net result of the Fourier synthesis approach is still an electron density strip model.

The model approach requires one to first choose a possible model. Physical (electron microscopy and birefringence) and chemical (composition, density) data provide certain information which can be utilized in choosing such a model. The point of view expressed in this paper is that a study of the $J_{obs}(h)$ data compared to possible model transforms, together with a study of the Patterson function, can sometimes directly lead to a choice of a suitable model.

Once a model is chosen it can be tested by computing the R-value:

$$R = \frac{\sum |[J'_{calc}(h)]^{1/2} - [KJ_{obs}(h)]^{1/2}|}{\sum [KJ_{obs}(h)]^{1/2}}. \tag{14}$$

If the model fits the X-ray data then the magnitude of the R-value should be close to the magnitude of the error in obtaining $[J_{obs}(h)]^{1/2}$. The question of whether the chosen model is, in fact, the correct one cannot be easily answered. Two points are noted: the chosen model should show a sharp minimum in R-value as the model parameters are varied and all features of the chosen model should be in keeping with known physical and chemical data. We note, in the case of a particular model, even if these two points are valid, that this does not necessarily constitute a proof of correctness. However, in practice, a chosen model which has a small R-value and which does not contradict known physical and chemical data is assumed to be a good approximation to the correct one.

ELECTRON DENSITY STRIP MODELS

Consider a centrosymmetric model of length d which has n electron density strips from $x = 0$ to $x = x_n = d/2$. The origin is chosen at $x = 0$ as shown in Fig. 1. The first strip of width x_1 has uniform electron density t_1, the second strip of width $x_2 - x_1$ has uniform electron density t_2, and the jth strip of width $x_j - x_{j-1}$ has uniform electron density t_j. In an n-strip model (each with different electron densities) there are $2n - 1$ model parameters. We require the number of the experimental parameters h to exceed $2n - 1$, the number of model parameters. This insures a reasonable test of the model transform against the $J_{obs}(h)$ values. The maximum value of h is moderately large in some cases, for example, collagen $h \approx 25$ (Tomlin and Worthington, 1956) or nerve myelin $h \approx 12$ (Blaurock and Worthington, to be published) so that fairly detailed models can be put forward on the basis of the low-angle X-ray data. From equation 2 it follows that the Fourier transform of an n-strip model is given by

$$T(X) = 2\sum_{j=1}^{j=n} t_j[x_j \operatorname{sinc} 2\pi X x_j - x_{j-1} \operatorname{sinc} 2\pi X x_{j-1}]. \tag{15}$$

This formula has been used in relation to models for collagen (Worthington, 1955), mitochondria (Worthington, 1960), nerve myelin (Finean and Burge, 1963), and cell wall of bacteria (Burge and Draper, 1967).

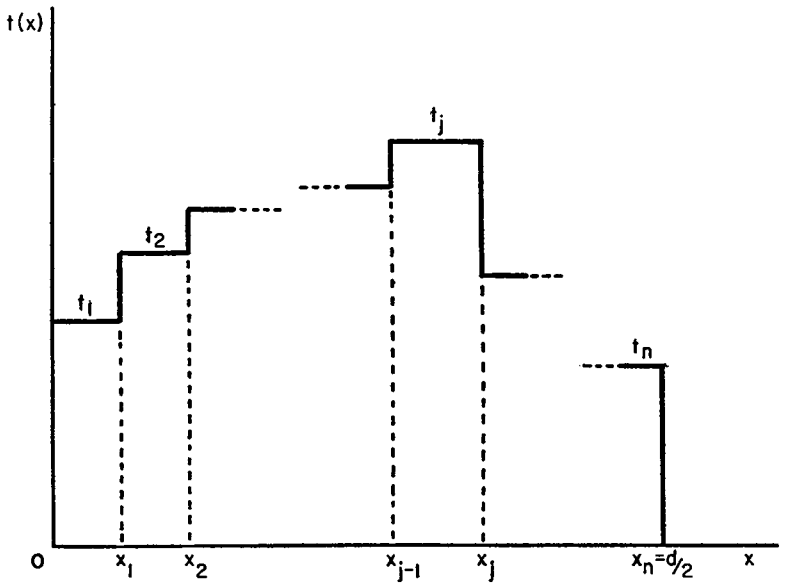

FIGURE 1 Centrosymmetric n-strip electron density model has n uniform electron densities $(t_1, t_2, \cdots t_j \cdots t_n)$ in n strips of width $(x_1, x_2 - x_1, \cdots x_j - x_{j-1}, \cdots x_n - x_{n-1})$.

Formula 15 can be rearranged in the following way. Denote $\bar{x}_j = \frac{1}{2}[x_j + x_{j-1}]$ where $\bar{x}_j$ is the distance from the origin to the center of the jth strip and $v_j = x_j - x_{j-1}$ where v_j is the width of jth strip. Formula 15 becomes

$$T(X) = 2\sum_{j=1}^{j=n} t_j v_j \operatorname{sinc} \pi X v_j \cos 2\pi X \bar{x}_j . \tag{16}$$

Formula 16 can be interpreted as electron densities $[t_j v_j \operatorname{sinc} \pi v_j X]$ placed at centers $\bar{x}_j$. We note that $\operatorname{sinc} \pi vX \approx \exp\{-\frac{1}{2}\pi(2X)^2\}$ provided $vX < 1$ and therefore Gaussian electron densities placed at $\bar{x}_j$ have approximately the same Fourier transform as uniform electron densities confined to strips (with centers $\bar{x}_j$). Differences will be apparent at large X, that is, when $vX > 1$.

In the general case the determination of a n-strip model from the observed $J_{obs}(h)$ values is not easily achieved. However, low-angle X-ray data from certain biological membrane-type structures suggest that a n-strip model with $n \approx 3$ or 4 may suffice to give agreement with the observed data. We next describe the Fourier transforms for eight special membrane-type models.

SPECIAL STRIP MEMBRANE-TYPE MODELS

The simplest model assumes that the membrane has uniform electron density M and width u. The next level of sophistication is to adopt the familiar triple layered unit which has lipid of electron density L of width l with nonlipid of electron density P of width p on the outer surfaces of the lipid; $u = 2p + l$ and $M = 1/u(2pP +$

TABLE I

MODEL PARAMETERS FOR (1) THE UNIFORM DENSITY MEMBRANE UNIT AND (2) THE TRIPLE LAYERED UNIT

(1) *a.* $t_1 = M$, $x_1 = u/2 = d/2$.
b. $t_1 = M$, $x_1 = u/2$; $t_2 = R$, $x_2 = d/2$.
c. $t_1 = M$, $x_1 = w/2 = d/2$.
d. $t_1 = M$, $x_1 = w/2$; $t_2 = R$, $x_2 = d/2$.

(2) *a.* $t_1 = L$, $x_1 = l/2$; $t_2 = P$, $x_2 = u/2 = d/2$.
b. $t_1 = L$, $x_1 = l/2$; $t_2 = P$, $x_2 = u/2$; $t_3 = R$, $x_3 = d/2$.
c. $t_1 = P$, $x_1 = p$; $t_2 = L$, $x_2 = p + l$; $t_3 = P$, $x_3 = w/2 = d/2$.
d. $t_1 = P$, $x_1 = p$; $t_2 = L$, $x_2 = p + l$; $t_3 = P$, $x_3 = w/2$; $t_4 = R$, $x_4 = d/2$.

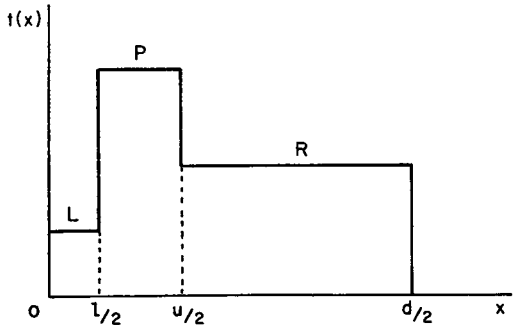

FIGURE 2 Diagram of model (2)*b* showing a single triple-layered unit of width u in medium R.

lL). There are four arrangements of each to consider: (*a*) by itself; (*b*) in medium R; (*c*) two membrane units together (a membrane pair, $w = 2u$); (*d*) a membrane pair in medium R. The model parameters are given in Table I where (1) refers to the simple M unit and (2) refers to the triple-layered unit. Models (2)*b* and (2)*d* are shown in Figs. 2 and 3, respectively. The values of $T(0)$ are the same for (1) and (2), these are:

a. $T(0) = Md$

b. $T(0) = (M - R)u + Rd$

c. $T(0) = Md$

d. $T(0) = (M - R)w + Rd$.

The expressions for $T'(X)$, $X = h/d$ follow from equation 15 and are given in Table II.

A model that is often used in reference to the four models with medium R, that is, (1)*b*, (1)*d*, (2)*b*, and (2)*d* is $\Delta t(x) = t(x) - R$. For instance, model $\Delta t(x)$ for case (1)*b* has electron density $(M - R)$ within the membrane unit and vacuo within the space $(d - u)$. We note $\Delta T'(X) = T'(X)$ and, therefore, models $\Delta t(x)$ and $t(x)$

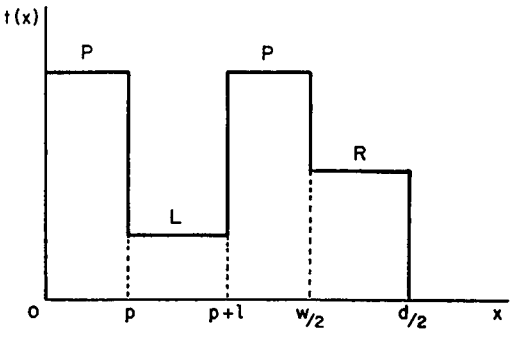

FIGURE 3 Diagram of model (2)*d* showing two triple-layered units joined together to form a pair of width $w = 2u$ in medium *R*.

TABLE II

EXPRESSIONS FOR $T'(X)$, $X = h/d$ FOR (1) THE UNIFORM DENSITY MEMBRANE UNIT AND (2) THE TRIPLE-LAYERED UNIT

(1) *a*. $T'(X) = 0$, that is, no diffraction.
b. $T'(X) = (M - R)u \operatorname{sinc} \pi uX$.
c. $T'(X) = 0$.
d. $T'(X) = (M - R)w \operatorname{sinc} \pi wX$.

(2) *a*. $T'(X) = -(P - L)l \operatorname{sinc} \pi lX$.
b. $T'(X) = -(P - L)l \operatorname{sinc} \pi lX + (P - R)u \operatorname{sinc} \pi uX$.
c. $T'(X) = -(P - L)l[2(p + l) \operatorname{sinc} \pi 2(p + l)X - 2p \operatorname{sinc} \pi 2pX]$.
d. $T'(X) = -(P - L)l[2(p + l) \operatorname{sinc} \pi 2(p + l)X - 2p \operatorname{sinc} \pi 2pX] + (P - R)w \operatorname{sinc} \pi wX$.

cannot be distinguished on the basis of $J_{obs}(h)$ alone. However $\Delta T(0) = T(0) - Rd$ so that $\Delta T(X) \neq T(X)$.

Swelling or shrinkage phenomena can be described by the four models with medium *R*, that is, (1)*b*, (1)*d*, (2)*b*, and (2)*d*. Consider model (1)*b*, exchange medium *R* for *S*, record a new period *g*; assume *M* and *u* are unchanged, then from Table II, $S'(X) = (M - S)u \operatorname{sinc} \pi uX$, $X = h/g$ and the difference transform $S'(X) - T'(X)$ is given by

$$S'(X) - T'(X) = (R - S)u \operatorname{sinc} \pi ux. \tag{17}$$

This method allows the width *u* to be derived. The method was first applied to crystals of hemoglobin (Boyes-Watson and Perutz, 1943). We note that the difference between the salt-free and salt Fourier transforms for hemoglobin given by Perutz (1954) when reduced to one-dimension is identical to the difference term in equation 17.

Consider the case of some planar structure of width *u* interspaced with a liquid layer of width $d - u$. The planar structure may have a complicated electron density variation such that models (1)*b* and (2)*b* do not apply. However, at very small angles of diffraction model (1)*b* can be a fair approximation: $T'(X) = (M - R)u \operatorname{sinc} \pi uX$. We assume knowledge of *R* and if *M* is known, then *u* can be estimated,

or alternatively, if u is known, then M can be estimated. If R can be changed, then both M and u can be estimated. We note when $M - R = 0$ $T'(X) = 0$, a well-known result in the theory of X-ray diffraction.

In summary, the Fourier transform of any proposed model can be calculated and $J'(h)$ values compared to the $J_{obs}(h)$ values. The observed $J_{obs}(h)$ values may trace out a well-defined pattern with zeroes at certain values of reciprocal space (see, for example, the nerve myelin pattern, Worthington and Blaurock, 1968). Various model parameters may be chosen in order that the model transforms show the same pattern of zeroes. Systematic analysis along these lines will vary with the proposed model, but this procedure is one way of choosing model parameters.

NORMALIZATION CONSTANT K

The normalization constant K can be determined on the basis of an electron density strip model by using Parseval's Theorem:

$$\int_{-\infty}^{\infty} J(X)\, dX = \int_{0}^{d} t^2(x)\, dx, \tag{18}$$

where $P(0) = \int_0^d t^2(x)\, dx$. We approximate the integral on the left-hand side of equation 18 by using the limits $\pm X_o$ and by using $KJ_{obs}(h) = J'(h)$, hence obtain an expression for K:

$$K = \frac{P(0) - 1/d\, J(0)}{P''(0)} \tag{19}$$

where $P''(0) = 2/d \sum_1^h J_{obs}(h)$ from equation 12. Hence K can be found on the basis of a model, provided $J(0)$ is known. This formula (with modifications) has been used to find K in liquids (Krogh-Moe, 1956; Norman, 1957) and in macromolecular systems (Blasie and Worthington, 1969).

The expressions for K for the special membrane-type models (1) and (2) are given in Table III.

TABLE III

EXPRESSION FOR THE NORMALIZATION CONSTANT K FOR MODELS (1) AND (2)

(1)	*a*. No diffraction.
	b. $KP''(0) = (M - R)^2(d - u)\, u/d$.
	c. No diffraction.
	d. $KP''(0) = (M - R)^2(d - w)\, w/d$.
(2)	*a*. $KP''(0) = (P - L)^2\, 2pl/d$.
	b. $KP''(0) = (P - L)^2\, 2pl/u + (M - R)^2(d - u)\, u/d$.
	c. $KP''(0) = (P - L)^2\, 8pl/d$.
	d. $KP''(0) = (P - L)^2\, 8pl/w + (M - R)^2\, (d - w)\, w/d$.

The analysis of low-angle data from normal and swollen biological tissues calls for the use of an absolute scale in order to compare $T'(x)$ and $S'(X)$, the normal and swollen Fourier transforms. Consider model (2)*d* which is thought to apply to nerve myelin (Worthington and Blaurock, 1968). Noting that $P > R > L$ the expression for K given in Table III has the property that $(P - L)^2 8pl/w \gg (M - R)^2(d - w)w/d$ and it is permissible to neglect this second term, that is, $(M - R)^2(d - w)w/d$. Hence

$$1/d\sum_{1}^{h} | T'(h) |^2 = 1/g\sum_{1}^{h} | S'(h) |^2, \tag{20}$$

a result which has been demonstrated experimentally in the case of nerve myelin (Worthington and Blaurock, to be published).

Patterson Analysis

The Patterson function $P''(x)$ given by equation 12 can be directly computed from the low-angle data $J_{obs}(h)$. If K and $J(0)$ can be found, then $P'(x)$ given by equation 11 can also be evaluated. Therefore, $P(x)$ from equation 9 can be determined from some model and compared with either $P''(x)$ or $P'(x)$ to see whether such a model might be an appropriate choice. In practice $P(x)$ from a strip model with large n is tedious to compute (by hand) and comparison with either $P''(x)$ or $P'(x)$ is not likely to be decisive.

However, some of the special membrane-type models have characteristic Patterson functions such that a study of $P''(x)$ may suffice to allow some model parameter to be chosen. The four models with medium R, that is (1)*b*, (1)*d*, (2)*b*, and (2)*d* are of interest. $P(x)$ or $\Delta P(x)$ can be calculated from some proposed model; however, $\Delta P(x)$ is the more convenient. From equation 9 $\Delta P(x) = \Delta t(x) * \Delta t(-x)$ and because $\Delta J'(h) = J'(h)$, hence

$$\Delta P(x) - 1/d\Delta J(0) = P(x) - 1/dJ(0), \tag{21}$$

so that $\Delta P(x)$ and $P(x)$ are simply related.

The determination of $\Delta P(x)$ is particularly straightforward when the models *b* and *d* are swollen, that is, *d* is large compared to either *u* or *w*. For instance, in case *d*, $\Delta P(x)$ then contains the autocorrelation of *w* with *w* to give a width *w* in the Patterson function from $x = 0$ to $x = w$. However, if $d < 2w$ in case *d*, then the self autocorrelation only holds from $x = 0$ to $x = x_o$ where $x_o = d - w$ and the Patterson function $\Delta P(x)$ from $x = x_o$ to $x = d/2$ contains overlapping terms which complicates the simpler self autocorrelation.

A description of $\Delta P(x)$ for the four models with medium R is as follows:
(1)*b*. Choose $d > 2u$. $\Delta P(x)$ falls linearly from its origin value at $x = 0$ to zero at $x = u$ and remains zero until $x = d/2$.

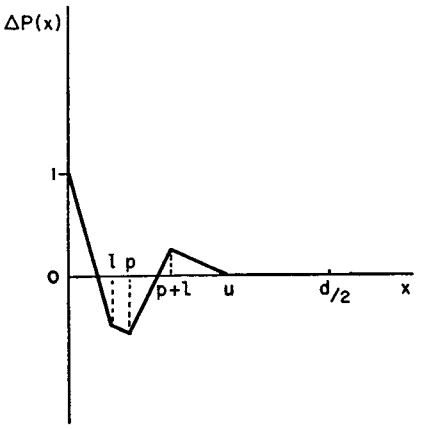

FIGURE 4 Patterson function $\Delta P(x)$ for model (2)*b* with the following parameters: $P = 0.38$, $R = 0.33$, $L = 0.25$ electrons/A^3; $p = 0.07d$, $l = 0.05d$, and $u = 0.19d$.

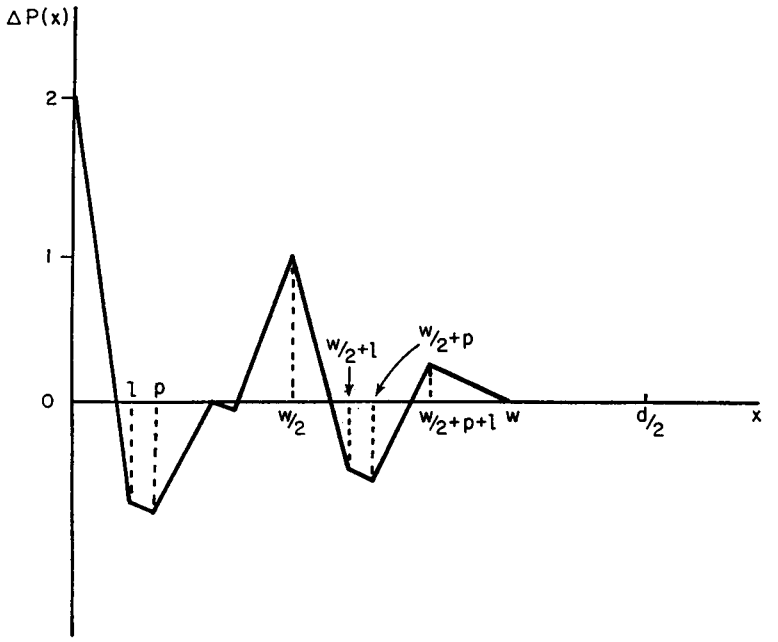

FIGURE 5 Patterson function $\Delta P(x)$ for model (2)*d* with the following parameters: $P = 0.38$, $R = 0.33$, $L = 0.25$ electrons/A^3; $p = 0.07d$, $l = 0.05d$, and $w = 0.38d$. The scale $\Delta P(x)$ is the same scale as in Fig. 4; we note the origin peak in Fig. 4 is one-half the origin peak in Fig. 5.

(1)*d*. Choose $d > 2w$. $\Delta P(x)$ falls linearly from its origin value at $x = 0$ to zero at $x = w$ and remains zero until $x = d/2$.

(2)*b*. Choose $d > 2u$. Let $P > R > L$ and $p > l$. $\Delta P(x)$ for this case is shown in Fig. 4. $\Delta P(x)$ has minima at $x = l$ and $x = p$ and a minor peak at $x = p + l$. The rapid origin fall-off is from $x = 0$ to $x = l$. $\Delta P(x)$ is zero from $u \leq x \leq d/2$.

If $l > p$, the minor peak again occurs at $x = p + l$ but the minima are interchanged; the rapid origin fall-off ends at $x = p$.

(2)*d*. Choose $d > 2w$. Let $P > R > L$ and $p > l$. $\Delta P(x)$ for this case is shown in Fig. 5. $\Delta P(x)$ has minima at $x = l$ and $x = p$ and a minor peak occurs at $x = p + l$ as in the single membrane model (2)*b*. However, a major peak occurs at $x = w/2$. Its peak height is half that of the origin peak, that is, $\Delta P(0) = 2\Delta P(w/2)$. The Patterson function from $x = w/2$ to $x = w$ is identical to that for the single membrane model but in the range of $x = 0$ to $x = u$. That is, minima occur at $x = w/2 + l$ and $x = w/2 + p$ and the minor peak occurs at $x = w/2 + p + l$. If $l > p$, then the minima are interchanged at $x = l$ and $x = p$, and at $x = w/2 + l$ and $x = w/2 + p$.

The Pattersons of our four swollen models show the following characteristic features:

(1)*b*. The linear fall-off ends at $x = u$ and, therefore, parameter u is determined.

(1)*d*. The linear fall-off ends at $x = w$ and, therefore, parameter w is determined.

(2)*b*. The minor peak occurs at $p + l$ and the rapid linear origin fall-off ends at either $x = p$ or $x = l$. Hence, either p or l, and $p + l$ is determined.

(2)*d*. The major peak occurs at $x = w/2$. Hence, parameter w is obtained. The rapid origin and major peak fall-offs both end at either $x = p$ or $x = l$ and hence, p or l is obtained. If the minor peak is resolved, then $p + l$ is also determined.

In summary the Patterson function $\Delta P(x)$ can be calculated for any proposed model and compared with either $P''(x)$ or $P'(x)$, if K and $J(0)$ are known. Both $P''(x)$ and $P'(x)$ have limited resolution and therefore, any identification of fine details in $\Delta P(x)$ with those of either $P''(x)$ or $P'(x)$ must be made with care. However, the identification of the stronger characteristic features should be apparent and, in particular, if the model under study is thought to be one of the above four membrane-type models, then certain model parameters can be directly determined.

CONCLUDING REMARKS

The analysis and the discussion given in this paper are aimed at finding an electron density strip model, not necessarily a complex one, but one that will give a good fit to the low-angle X-ray data. This model should contain the prominent and distinctive macrostructural electron density variations. In order to bring out finer details, additional model parameters may have to be added depending on the amount of X-ray data available. This refinement procedure has not been treated.

The usefulness of a model, even though it is not a complex one, is that it gives a description of electron densities in the intact biological tissue. This description is most likely not perfect, but it may be in harmony with the information contained in the low-angle X-ray data. Any proposed molecular arrangement of components comprising the biological tissue should be in fairly close agreement with the favored model. This model may have fairly precise parameters which will strongly influence the possible ways of packing the molecular components.

I am indebted to former members of this laboratory, Drs. K. Blasie and A. Blaurock, for helpful discussion.

This work was supported by United States Public Health Service Grant GM-09796.

Received for publication 29 August 1968.

REFERENCES

BLASIE, J. K., M. M. DEWEY, A. E. BLAUROCK, and C. R. WORTHINGTON. 1965. *J. Mol. Biol.* **14**:143.
BLASIE, J. K., and C. R. WORTHINGTON. 1969. *J. Mol. Biol.* **39**: In press.
BLAUROCK, A. E., and C. R. WORTHINGTON. 1966. *Biophys. J.* **6**:305.
BOYES-WATSON, J., and M. F. PERUTZ. 1943. *Nature.* **151**:714.
BURGE, R. E., and J. C. DRAPER. 1965. *Lab. Invest.* **14**:978.
BURGE, R. E., and J. C. DRAPER. 1967. *J. Mol. Biol.* **28**:189.
FINEAN, J. B., and R. E. BURGE. 1963. *J. Mol. Biol.* **7**:672.
JAMES, R. W. 1948. The Crystalline State. G. Bell & Sons, Ltd., London, England.
KROGH-MOE, J. 1956. *Acta Cryst.* **9**:951.
LIPSON, H., and W. COCHRAN. 1953. The Crystalline State. G. Bell & Sons, Ltd., London, England. III.
NORMAN, N. 1957. *Acta Cryst.* **10**:370.
PERUTZ, M. F. 1954. *Proc. Roy. Soc., Ser. A (London).* **225**:264.
RAND, R. P., and V. LUZZATI. 1968. *Biophys. J.* **8**:125.
TOMLIN, S. G., and C. R. WORTHINGTON. 1956. *Proc. Roy. Soc., Ser. A (London).* **235**:189.
WORTHINGTON, C. R. 1955. Ph.D. Thesis. Adelaide University, Australia.
WORTHINGTON, C. R. 1960. *J. Mol. Biol.* **2**:327.
WORTHINGTON, C. R., and A. E. BLAUROCK. 1968. *Nature.* **218**:87.